論文 / 著書情報
Article / Book Information

Title	Quantitative control and detection of heterovalent impurities in ZnO thin films grown by pulsed laser deposition
Authors	M. Sumiya,S. Fuke,A. Tsukazaki,K. Tamura,A. Ohtomo,M. Kawasaki,H. Koinuma
Citation	Journal of Applied Physics, Vol. 93, No. 5,
発行日/Pub. date	2003, 5
公式ホームページ /Journal home page	http://jap.aip.org/
権利情報/Copyright	Copyright (c) 2003 American Institute of Physics

Quantitative control and detection of heterovalent impurities in ZnO thin films grown by pulsed laser deposition

M. Sumiya[a] and S. Fuke
Department of Electrical and Electronic Engineering, Shizuoka University, Hamamatsu 432-8561, Japan

A. Tsukazaki, K. Tamura, A. Ohtomo, and M. Kawasaki
Institute for Materials Research, Tohoku University, Sendai 980-8577, Japan

H. Koinuma[b]
Materials and Structures Laboratory, Tokyo Institute of Technology, Yokohama, 226-8502, Japan

(Received 22 August 2002; accepted 9 December 2002)

Impurities in ZnO specimens, including targets for pulsed laser deposition and thin films resulting from their use, were analyzed by secondary ion mass spectroscopy (SIMS). Negatively charged complex ions bound with oxygen ($^{71}Ga^{16}O^-$ and $^{14}N^{16}O^-$) were found to be the most reliable species with which to evaluate the Ga and N content of ZnO films by clarifying possible mass interference effects in SIMS analysis. Calibrations were carried out to determine the Ga concentration (C_{Ga}) and the nitrogen concentration (C_N) by normalizing the signal intensities for $^{71}Ga^{16}O^-$ and $^{14}N^{16}O^-$, respectively, to that for $^{70}Zn^{16}O^-$. Alternative ablation of pure single crystal and Ga-doped ceramic ZnO targets was found to be effective not only for achieving systematic control of the Ga concentration in ZnO:(Ga,N) films, but also for minimizing the contamination of undesired impurities from the sintered targets. The substrate temperature plays a decisive role in control of C_N due to a thermally activated desorption process of N-related species during deposition. Systematic control of the C_N/C_{Ga} ratio in a ZnO:(Ga,N) film was carried out on a $ScAlMgO_4$ substrate by introducing a controlled temperature gradient on the substrate during deposition. A region with the correct concentration ratio of $C_N/C_{Ga}=2$, where *p*-type conduction of the ZnO film was theoretically predicted, was included in the composition spread sample in which the C_N/C_{Ga} ratio was continuously varied over a wide range. © *2003 American Institute of Physics.* [DOI: 10.1063/1.1542938]

I. INTRODUCTION

Highly efficient ultraviolet (390 nm) laser action at room temperature due to exciton recombination[1] has triggered intensive research into ZnO aimed at producing light emitting devices and lasers. Sophisticated band engineering is a mature technique which can be used to demonstrate even more efficient stimulated emission in ZnO/(Mg, Zn)O superlattices[2] and enhanced exciton coupling from 60 meV for bulk ZnO to 87 meV for the superlattices.[3] A critical issue to solve in order to achieve current injection devices is *p*-type doping of ZnO. By analogy with the case of ZnSe,[4] nitrogen doping has been carried out to produce *p*-type ZnO (Ref. 5, and references therein). Yamamoto *et al.* theoretically predicted that the codoping of Ga and N in a ZnO matrix with a concentration ratio of 1:2 would produce ZnO with high *p*-type[6] conductivity. Although several reports have claimed that *p*-type doping of ZnO is possible, it is still a controversial topic and a systematic study is needed, including accurate control and evaluation of the heterovalent impurity concentration.[5]

Secondary ion mass spectroscopy (SIMS) is the best tool by which to analyze impurity concentrations for valence control of semiconductors. However, the detection of nitrogen is very difficult even by SIMS, because the nitrogen atom is too stable to be ionized.[7] Therefore, it is necessary to perform careful analysis of ionic complex species, taking the natural abundance and mass interference effect into account. From our experiences of impurity measurement in GaN films by SIMS,[8] we expected that complex ions containing nitrogen would be a good measure of the nitrogen concentration in ZnO films.

In this article, we report on a systematic SIMS analysis of more than 700 ZnO specimens, including targets for pulsed laser deposition and the resulting films. The elements we were concerned with were Zn, Ga, and N. First, we will discuss the choice of ionic species for evaluating the concentrations, avoiding mass interference effects, and technical limitations. The choice of $^{70}Zn^{16}O^-$ for Zn (discussed in Sec. III A1), $^{71}Ga^{16}O^-$ for Ga (in Sec. III A2), and $^{14}N^{16}O^-$ for N (in Sec. III A3) are justified through careful examination. The calibration of absolute concentrations for Ga (C_{Ga}) and N (C_N) is shown using SIMS data for Ga-doped ZnO bulk ceramic specimens and N-implanted single crystal specimens, respectively. Then, we will show how C_{Ga} and C_N can be controlled systematically and independently by the correct choice of target ablation sequence and substrate temperature

[a]Author to whom correspondence should be addressed; electronic mail: temsumi@ipc.shizuoka.ac.jp
[b]Also at Combinatorial Materials Exploration and Technology (COMET), 169-0072, Japan.

TABLE I. SIMS count distribution ($m/e=80-88$) normalized to that of $m/e=86$ for all targets. – indicates signal intensity of over 1×10^6 counts. Zn isotopes: ^{64}Zn:^{66}Zn:^{67}Zn:^{68}Zn:^{70}Zn=48.6:28:4.1:19:0.6%; O isotopes: ^{16}O:^{17}O:^{18}O=99.76:0.04:0.2%; Ga isotopes: ^{69}Ga:^{71}Ga=60.1:39.9%; N isotopes: ^{14}N:^{15}N=99.63:0.37%.

m/e	80	81	82	83	84	85	86	87	88
Isotope combination	$^{64}Zn^{16}O^-$	$^{64}Zn^{17}O^-$	$^{66}Zn^{16}O^-$ $^{64}Zn^{18}O^-$	$^{67}Zn^{16}O^-$ $^{66}Zn^{17}O^-$	$^{68}Zn^{16}O^-$ $^{67}Zn^{17}O^-$ $^{66}Zn^{18}O^-$	$^{67}Zn^{18}O^-$ $^{68}Zn^{17}O^-$	$^{70}Zn^{16}O^-$ $^{68}Zn^{18}O^-$	$^{70}Zn^{17}O^-$	$^{70}Zn^{18}O^-$
Ideal intensity	76	0.031	43.9	6.4	29.8	0.025	1	0.00038	0.0019
EP target	–	0.042	–	5.8	–	0.030	1	0.0010	0.0019
(Ga-doped) 4×10^{19} cm^{-3} target	–	0.18	–	5.9	–	0.48	1	0.27	0.0030
2×10^{20} cm^{-3} target	–	0.068	–	6.0	–	2.2	1	1.5	0.0027
4×10^{20} cm^{-3} target	–	0.11	–	5.9	–	3.1	1	2.1	0.0043
2×10^{21} cm^{-3} target	–	0.48	–	6.2	–	–	1	–	0.017
Possible impurity species		$^{69}GaC^-$		$^{69}Ga^{14}N^-$		$^{69}Ga^{16}O^-$	$^{69}Ga^{17}O^-$	$^{71}Ga^{16}O^-$ $^{69}Ga^{18}O^-$	$^{64}Zn+2C^-$ $^{71}Ga^{18}O^-$

in Secs. III B and III C, respectively. Finally, we will demonstrate a way to adjust the dopant concentration ratio (C_N/C_{Ga}) to be exactly two by using an original temperature gradient method that we have developed, described in Sec. III C.

II. EXPERIMENTS

A. Sample preparation

We employed three kinds of specimens: high-purity single crystals made by a vapor transport method [Eagle Pitcher Co. (EP) target], sintered ceramics targets and epitaxial thin films. The former two were used as targets for producing epitaxial thin films by pulsed laser deposition. The impurity concentration for the EP target was reported to be Ga: 80 ppb, N: 100 ppb Al: 26 ppb, and Si: 530 ppb. The sintered ceramic targets were doped with a prescribed concentration of Ga that varied from 4×10^{19} (0.1 at. %) to 2×10^{21} cm^{-3} (5 at. %), as shown in Table I. These were analyzed by SIMS to produce a calibration curve for C_{Ga}. Since the ceramic targets were prepared by a conventional solid-state reaction, contamination with undesired impurities such as Al and Si was expected. The standard samples for C_N calibration were prepared by nitrogen ion implantation at 100 keV into an EP target (peak C_N: 1.8×10^{21} cm^{-3}) as well as into ZnO films on Al_2O_3 substrates (peak C_N: $3.1\times10^{18}-3.1\times10^{20}$ cm^{-3}).

Thin films were deposited on $ScAlMgO_4$ (0001) substrates[9] by pulsed laser deposition employing a KrF laser pulse (248 nm, 30 ns, 10 Hz) at oxygen pressure of either 10^{-5} or 10^{-6} Torr. To control the Ga concentration in the films, an EP target and a Ga-doped ceramic target were alternatively ablated at a prescribed ratio, as will be discussed in Sec. III B. When nitrogen was to be doped into the ZnO film, a radio frequency (rf) radical source gun (SVT Co.) was operated at 500 W with nitrogen gas flow of 3×10^{-5} Torr during pulsed laser deposition. The substrate was heated by radiation from a continuous wave semiconductor laser beam ($\lambda=804$ nm, 30 W).[5,10] Any additional experimental details are described in each section.

B. SIMS analysis

For SIMS analysis we employed a magnetic-sector-based instrument (Cameca IMS-4f). A Cs^+-ion beam was used as the primary ion source to detect negative secondary ions, since negative secondary ions were found to be more sensitive for detecting impurities. The primary beam energy was set at 14.5 kV and the current was approximately 20 nA. The primary beam was rastered within a 150 μm sq area, and the secondary ions were collected from the center of the rastering area through a physical aperture. The mass spectra were measured for mass number (m/e), ranging from 0.5 to 200 amu, while discriminating into 4000 channels using an integration time of 0.2 s per channel. The mass number is defined as m/e, where m is the mass of the ionic species and e is the electron charge. The most suitable mass number set was selected to determine the concentrations of Ga and N, as discussed in Sec. III A. Actual analyses were carried out by taking the depth profiles of the ionic species with a gate time of 1 s per channel for each mass number. The detector in our SIMS system is automatically switched from an electron multiplier to a Faraday cup when the integrated count exceeds 10^6 counts during the gate time. Therefore, we have to avoid mass numbers with very high signal intensity in the choice of ionic species. Also, for the choice of mass numbers that can be used to determine the Zn, Ga, and N species, we have to take into account the mass interference effect, whereby the intensity of one mass number overlaps that of

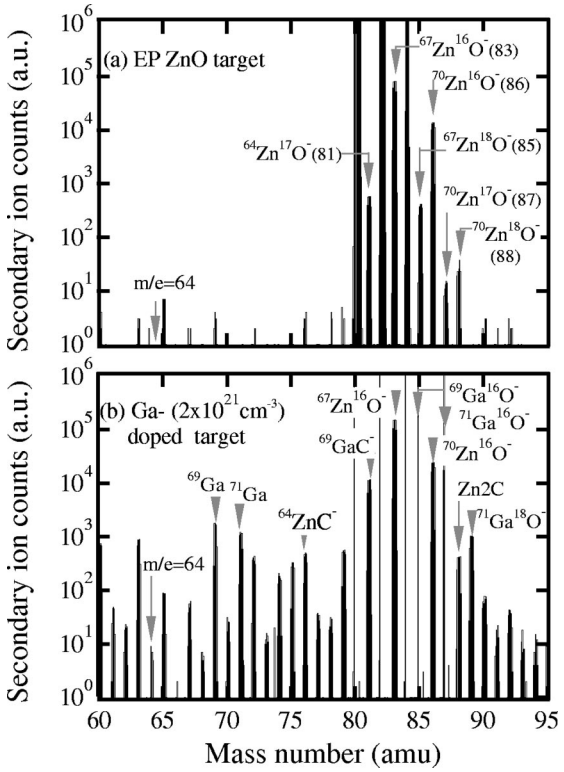

FIG. 1. Mass spectra for mass numbers ranging from 60 to 95 detected by SIMS using a Cs^+ primary beam for (a) an EP target and (b) a Ga-doped (2×10^{21} cm^{-3}) ceramic target. The peaks that we are concerned with are assigned as listed in Table I, taking into account their natural abundance and mass interference effects.

another species with the same m/e originating from a combination of isotopes or impurities in the matrix.

III. RESULTS AND DISCUSSION

A. Quantitative calibration of C_{Ga} and C_N in the ZnO matrix

1. Zn species

Figure 1(a) shows the mass spectrum for an EP target taken after removing the surface contamination by sputtering the surface to a depth of about 1.5 μm. The intensity distribution for the Zn isotopes ($m/e=64$–70) does not correlate with the natural abundance and the signals are almost in the noise level, even for the dominant isotope where $m/e=64$. However, the ZnO^- ($m/e=80$–88) complex ions listed in Table I show much higher intensities. The m/e values of 80, 82 and 84, which contain complex ions of high natural abundance such as $^{64}Zn^{16}O^-$, $^{66}Zn^{16}O^-$, and $^{68}Zn^{16}O^-$, respectively, should be avoided during the analysis because the signal intensity exceeds the limit of the electron multiplier detector. Therefore, the other ZnO^- species are good candidates as Zn-related species for evaluating impurity concentrations. Since Ga is next to Zn in the Periodic Table, we have to examine carefully the mass interference effect due to its isotopes. In Table I, the signal intensities for various m/e values (80–88) are listed, normalized to that for $m/e=86$. The ideal signal intensities are also listed based on the natural abundance of Zn and O, without taking into account the mass interference effect due to the presence of the Ga dopant and *C* contamination.

The mass spectrum of a Ga-doped ceramic target exhibits many additional peaks around the m/e value that we are concerned with, as shown in Fig. 1(b). The results for four Ga-doped ceramics are also listed in Table I. When $m/e=85$ or 87, which also corresponds to $^{69}Ga^{16}O^-$ and $^{71}Ga^{16}O^-$, respectively, the signal intensity increases as the Ga concentration in the target (C_{Ga}^{target}) increases. Therefore, these two m/e peaks cannot be used as a way of measuring a Zn-related signal, although they are useful to determine C_{Ga}, as will be discussed in Sec. III A2. For $m/e=81$ and 88, the signal intensity is so weak that the mass interference effect due to carbon contamination may become dominant. As a result, the signals for $m/e=83$ or 86 could be useful. Since the intensity of $m/e=83$ ($^{67}Zn^{16}O^-$) is close to the technical limit of 10^6 counts when the gate time is enlarged for the analysis of depth profiles, we decided to use an intensity of $m/e=86$($^{70}Zn^{16}O^-$) as the matrix signal. The mass interference effect due to $^{69}Ga^{17}O^-$ is confirmed as negligible due to the very low natural abundance of ^{17}O.

2. Ga species

In order to make a calibration curve to determine C_{Ga} in the thin films, we analyzed the four ceramic targets listed in Table I. The depth profiles for $^{70}Zn^{16}O^-$ and the Ga-related species [$m/e=69$ ($^{69}Ga^-$), 85 ($^{69}Ga^{16}O^-$), and 87 ($^{69}Ga^{18}O^-$)] were measured at several points in each Ga-doped target. The intensity for each mass number was almost constant throughout the depth profile analysis, and the intensity of $^{70}Zn^{16}O^-$ for each target was constant at $\sim2\times10^5$ counts. A smaller physical aperture was used to measure the target with the highest doping concentration (C_{Ga}^{target}:2.0×10^{21} cm^{-3}) to keep the signal intensity below 10^6 counts. Figure 2 shows the signal intensities for the above-mentioned species normalized to that of $^{70}Zn^{16}O^-$. For all of the species, the SIMS signal scales linearly with the prescribed doping concentration. However, the use of $m/e=69$ is not suitable because the signal intensity drops below the detection limit when we need to measure C_{Ga} below 1×10^{19} cm^{-3}. Although the choice of Ga complex ions seems to be suitable for quantitative analysis of C_{Ga} at less than 1×10^{18} cm^{-3}, we need to consider the mass interference effect due to the ZnO^- species. As shown in Table I, the signals originating from $^{67}Zn^{18}O^-$($m/e=85$) and $^{70}Zn^{17}O^-$($m/e=87$) overlap the signals for $^{69}Ga^{16}O^-$($m/e=85$) and $^{71}Ga^{16}O^-$($m/e=87$), respectively. Taking their natural abundance into account, the former contribution is much higher than the latter. By taking the mass interference effect into account as well, we simulated the possible profiles as a function of the Ga concentration and plotted them as dotted lines in Fig. 2. The former m/e value gives a considerable signal offset at lower C_{Ga}^{target}. Therefore, we concluded that the choice of $^{70}Zn^{17}O^-$($m/e=87$) would be the best for determining C_{Ga}. The ratio (x) of the signal intensity for $^{71}Ga^{16}O^-$($m/e=87$) to that for $^{70}Zn^{16}O^-$($m/e=86$) is the best choice with which to determine C_{Ga} in ZnO. The calibration equation deduced from Fig. 2 is given as

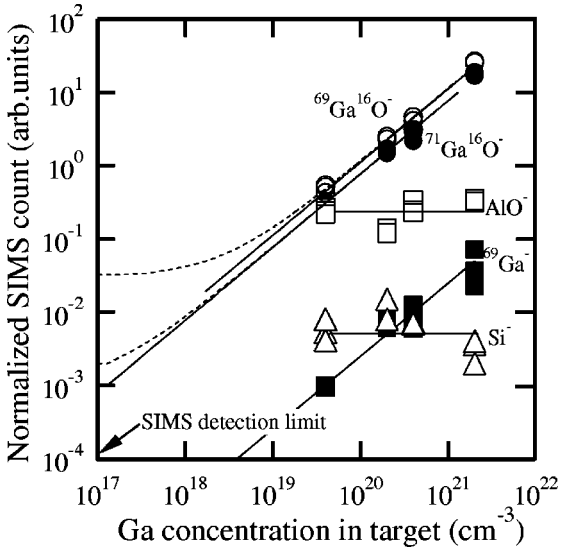

FIG. 2. Relationship between prescribed Ga concentrations in ceramic targets and SIMS counts for $^{69}Ga^-(m/e=69)$, $^{69}Ga^{16}O^-(m/e=85)$, $^{71}Ga^{16}O^-(m/e=87)$, $^{27}Al^{16}O^-(m/e=43)$, and $^{28}Si^-(m/e=28)$ normalized to that of $^{70}Zn^{16}O^-(m/e=86)$. The dotted lines are simulated by taking into account the contributions of $^{67}Zn^{18}O^-$ and $^{70}Zn^{17}O^-$, which have the same mass numbers as the Ga-related signals.

$$C_{Ga}=x\times 1.3\times 10^{20}\ \text{cm}^{-3}. \quad (1)$$

The lower limit for quantitative evaluation of C_{Ga} based on Eq. (1) is $\sim 5\times 10^{17}$ cm^{-3}, which is sufficient for practical doping experiments for thin films.

3. N species

We analyzed ZnO standard samples into which nitrogen ions had been implanted at an acceleration voltage of 100 kV. The dose quantity was varied over the range of 5×10^{13}–3×10^{16} cm^{-2}. Figure 3 shows depth profiles of the standard samples. The $^{70}Zn^{16}O^-$ ($m/e=86$) signal intensity is constant throughout the depth profile. Although a distinct peak appeared in the mass spectrum at $m/e=14$, the depth profile of the signal intensity for $m/e=14$ did not correlate with the C_N profile expected from ion implantation, suggesting impurity species such as CH_2^-. On the other hand, the depth profile of the complex ionic species $^{14}N^{16}O^-$ shows a clear Gaussian-like peak. According to theory,[11] the peak depth (L) and the standard deviation (σ) of the Gaussian distribution for nitrogen in the single crystal (dose: 3×10^{16} cm^{-2}) should be evaluated as 174 and 64 nm, agreeing with the experimental results. Therefore, given the dose quantity and the acceleration voltage, a complete Gaussian profile can be simulated. For example, for the highest dose

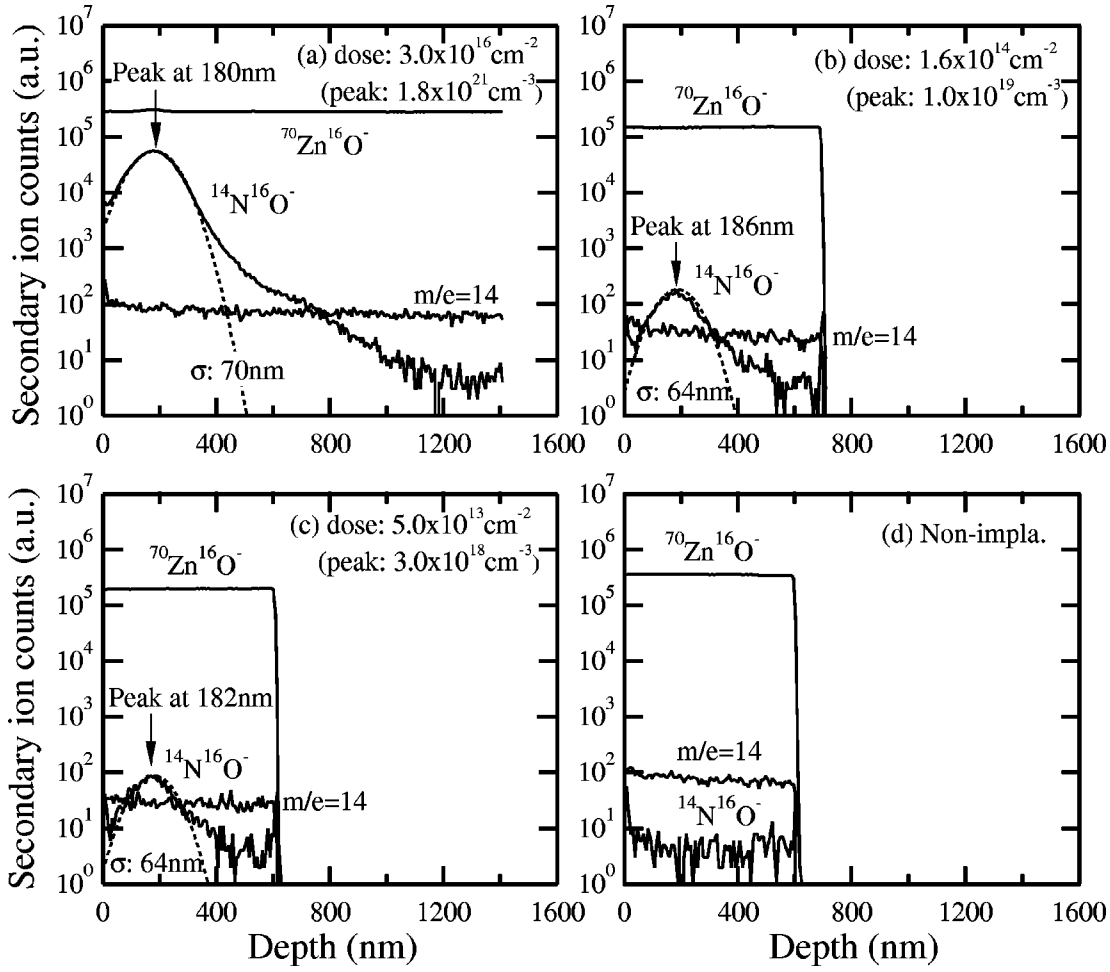

FIG. 3. Depth profiles of $^{70}Zn^{16}O^-$ and $^{14}N^{16}O^-(m/e=30)$ and $m/e=14$ for N ion-implanted standard ZnO epitaxial samples. Dose quantity: (a) 3×10^{16}, (b) 1.6×10^{14}, and (c) 5×10^{13} cm^{-2}, and (d) nonimplanted ZnO film. The calculated profiles of $^{14}N^{16}O^-$ are represented by the dotted lines.

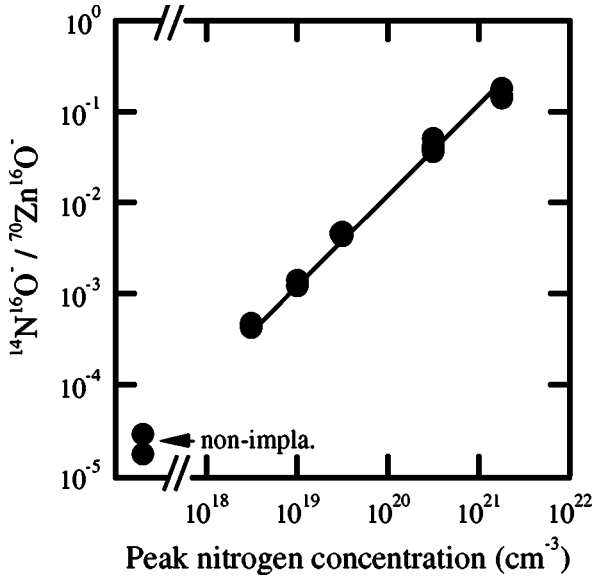

FIG. 4. Relationship between the peak nitrogen concentration and the intensity of $^{14}N^{16}O^-$ normalized to that of $^{70}Zn^{16}O^-$ for the standard samples. The intensity for the nonimplanted ZnO film is also plotted.

specimen, fitting (dotted line) resulted in $L=180$ nm and $\sigma=70$ nm, which are close to the expected values. The $^{14}N^{16}O^-$ profiles for the other standard samples could be also fit well by using the theory. Thus, we conclude that $m/e=30$ is the best choice for determining C_N in ZnO films.

When the peak intensities of $^{14}N^{16}O^-$, normalized to those of $^{70}Zn^{16}O^-$ (y) in the standard samples are plotted against the implanted peak concentrations, a clear linear relationship is obtained, as shown in Fig. 4. We determined the calibration curve for C_N in ZnO films from this relationship as

$$C_N(y)=y\times 0.9\times 10^{22}\ (\mathrm{cm}^{-3}). \tag{2}$$

Since the normalized intensity of $m/e=30$ for the nonimplanted ZnO film was $\sim 4\times 10^{-5}$, we conclude that the detection limit for C_N is as low as $\sim 4\times 10^{17}$ cm^{-3}, which is sensitive enough to use to determine C_N in doping experiments for these films. Therefore, $^{70}Zn^{16}O^-$, $^{14}N^{16}O^-$, and $^{71}Ga^{16}O^-$ can be used to determine C_N and C_{Ga} in ZnO:(Ga,N) films using a Cs^+ primary beam.

B. Control of concentrations for undesired impurities and Ga

One of the drawbacks of pulsed laser deposition compared with other semiconductor thin film deposition techniques such as molecular beam epitaxy and metalorganic chemical vapor deposition is that undesired impurities in the source materials are directly transformed into the thin films. The latter two methods involve a purification process of distillation during thermal evaporation of source materials. Therefore, the selection of highly pure targets is essential to make semiconductor thin films by pulsed laser deposition. In this sense, the EP target is very suitable as one of the source materials. However, as shown in Fig. 2, Ga-doped ceramic targets contain high levels of impurities such as Al and Si, both of which act as electron donors in ZnO. Also, it is practically impossible to prepare ceramic targets that have the prescribed C_{Ga}^{target} below 0.1 at. %. To solve these problems, we propose here an alternative ablation technique using a high purity EP target and Ga-containing ceramic targets to minimize undesired impurities and to regulate C_{Ga} at low doping levels.

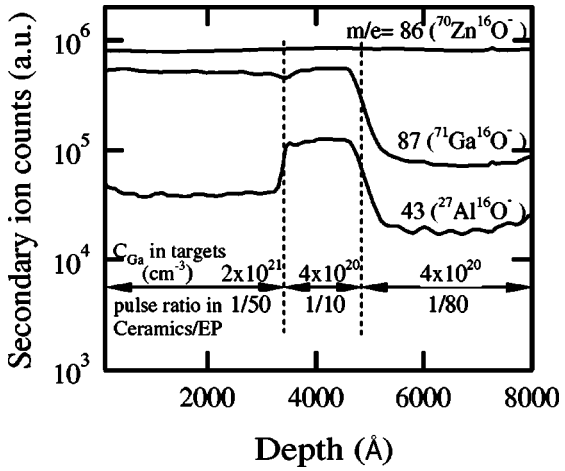

FIG. 5. Depth profiles of $^{70}Zn^{16}O^-$, $^{71}Ga^{16}O^-$, and $^{27}Al^{16}O^-$ species for the accumulated trilayer sample deposited using different Ga-doped ceramic targets and the pulse ratio sequence indicated.

Figure 5 shows the depth profile of a sample composed of three layers grown by different target switching sequences in an alternative ablation technique. The bottom layer was grown by repeated cycles of 1 pulse ablation of a Ga-containing ceramic target (C_{Ga}^{target}:4.0×10^{20} cm^{-3}) and 80 pulse ablation of an EP target. The middle layer was grown with a pulse ratio of 1:10 with the same set of targets. The top layer was grown with a pulse ratio of 1:50 using another Ga-containing ceramic target (C_{Ga}^{target}:2.0×10^{21} cm^{-3}). Note that the typical deposition rate of the films is 0.01 nm/pulse and it takes 26 pulses to form one molecular layer (0.26 nm) of ZnO. Therefore, the alternating ablation technique can be considered to create a uniform distribution of dopants.

The profile of C_{Ga} ($m/e=87$) can be well regulated by changing the pulse ratio and Ga concentration in the targets. C_{Ga} is kept constant from the top to the middle layers. C_{Ga} for the bottom layer is lower than for the top (and middle) layer by a factor of about 8. The profile of $^{27}Al^{16}O^-$ ($m/e=43$), one of the undesired impurities, varies in proportion to the pulse ratio. This means that the Al-related species are incorporated mainly from the ceramic targets.

To clarify these effects, we carried out some more systematic experiments. The growth conditions for the films are summarized in Table II. Although the substrate temperature chosen was varied in order to regulate C_N, as discussed later, this variation has little influence for the discussion here. We defined the designed Ga concentration ($C_{Ga}^{calculate}$) as simply the product of the ablating pulse ratio and C_{Ga}^{target} in the target. Figure 6 shows the actual C_{Ga} in the films and the normalized signal intensities for $^{27}Al^{16}O^-$ and $^{28}Si^-$ as a function of $C_{Ga}^{calculate}$. The C_{Ga} value can be successfully regulated by the choice of C_{Ga}^{target} and the pulse ratio, as can be seen by the scaling behavior in Fig. 6. Although a slight offset, by a factor of 2, is present (the difference between the solid and

TABLE II. Sample preparation conditions for the alternative ablation ratio of Ga-doped and EP targets. The calculated C_{Ga}^{calc} was simply evaluated from the ablation ratio and C_{Ga}^{target}. The oxygen pressure was 1×10^{-6} Torr. The rf power for the N radical was constant at 500 W, with N_2 gas flow of 3×10^{-5} Torr.

Temperature (°C)	C_{Ga}^{target} (cm^{-3})	Pulse ratio	C_{Ga}^{calc} (cm^{-3})
A 465–500	2×10^{21}	1/50	4×10^{19}
B 575–510	4×10^{20}	1/80	5×10^{18}
C 530–650	4×10^{20}	1/500	8×10^{17}

broken lines), this enrichment of Ga due to the volatile nature of the Zn-related species will be discussed later. The ceramic targets contain similar concentrations of Al and Si impurities, regardless of C_{Ga}^{target} in the targets, as shown in Fig. 2. Even the EP target shows a distinct peak in the mass spectrum, indicating that the peaks of $m/e=43$ and 28, respectively, may not represent solely Al- and Si-related impurities. Nonetheless, the expected signal intensities were calculated for these impurity peaks by taking into account the signal intensities in the targets and the ablation ratio to give the dotted lines. The signal intensities (open symbols) measured for these films after alternative ablation of these two targets agree well with those shown by the dotted line. Therefore, we conclude that the level of undesired impurities can be reduced by the alternative ablation scheme and approach those of the EP target. The undesired impurity concentrations in the films were decreased by almost two orders of magnitude compared with those in the Ga-doped ceramic targets.

C. Quantitative doping control of N

Unlike in the case of Ga incorporation, N incorporation strongly depends on the surface chemistry, i.e., the former

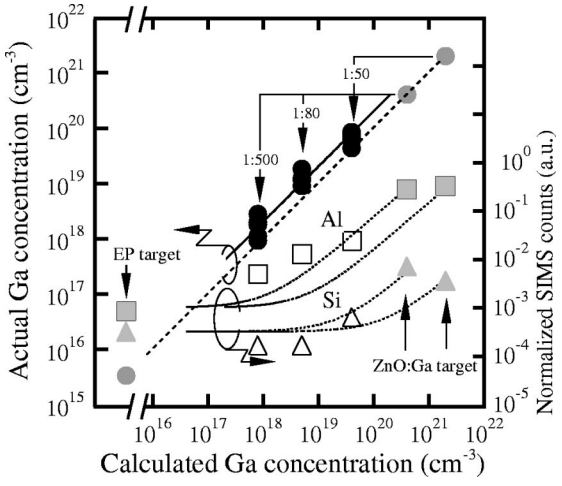

FIG. 6. Ga concentration (left axis), normalized $^{27}Al^{16}O^-$ (open square), and $^{28}Si^-$ (open triangle) counts (right axis) for the thin films deposited using different ceramic targets and the ablation ratios given in Table II as a function of the calculated Ga concentration. For reference, the concentration and the counts in the targets are given by the same symbols in and shown gray. The dotted lines are calculated for the intensities of $^{27}Al^{16}O^-$ and $^{28}Si^-$ impurities taking into account the signal intensities in the targets and the ablation ratio.

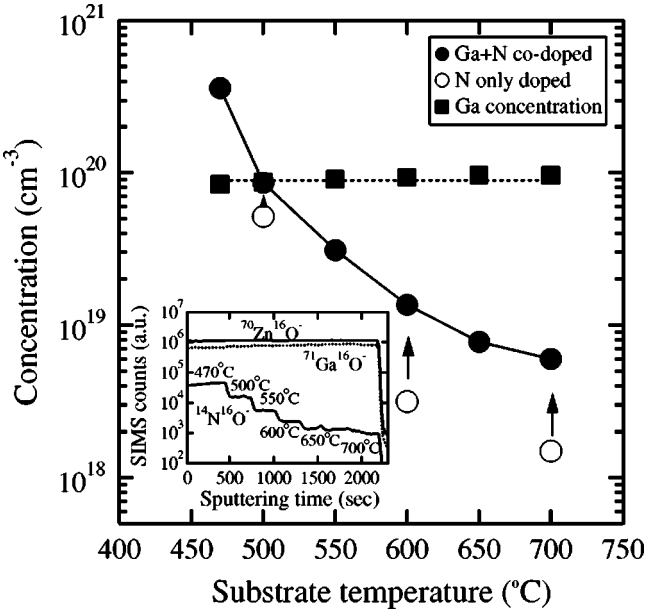

FIG. 7. Temperature dependence of N and Ga concentrations in a ZnO:N film grown by ablating an EP target (open circle) and a ZnO:(Ga,N) film deposited using ablation scheme A in Table II (closed symbols). Both samples were accumulated from high to low temperatures under the same nitrogen radical conditions. The depth profile of the ZnO:(Ga,N) sample is given in the inset.

can be simply controlled by C_{Ga}^{target} and the pulse ratio, as discussed above, due to similar sticking coefficients of close to unity for Zn- and Ga-related species. However, the level of N incorporation strongly depends on the substrate temperature, due to the thermally activated desorption of N-related species. Therefore, in order to discuss the N incorporation process in a quantitative fashion, we need to regulate the surface chemical reaction process and the resulting film crystallinity. To do this, the use of a lattice matched $ScAlMgO_4$ substrate is vitally important. As reported previously, excellent crystallinity can be achieved for ZnO on $ScAlMgO_4$, even at a substrate temperature as low as 150 °C.[9] The incorporation of N has hardly any deleterious effect on the crystallinity in the temperature range of 400–600 °C.[12] The results described here in Sec. III C are based on these results.

Figure 7 shows the temperature dependence of C_N in ZnO:N and C_N and C_{Ga} in ZnO:(Ga,N) films on $ScAlMgO_4$ substrates. The ZnO:N films were grown by ablating an EP target under constant irradiation with a N radical. The ZnO:(Ga,N) films were deposited using ablation scheme A in Table II under the same N radical conditions. The films were grown cumulatively at various temperatures, from high to low, so a depth profile through the stack could provide a series of data points. An example of a depth profile of a ZnO:(Ga,N) film is given in the inset of Fig. 7. For both cases of N doping, with and without the addition of a Ga dopant, C_N decreases exponentially when the substrate temperature increases whereas C_{Ga} is kept constant. It should be noted that C_N is apparently higher for ZnO:(Ga,N) than for ZnO:N, especially at higher growth temperatures. This finding should be correlated with the surface chemistry, i.e., the

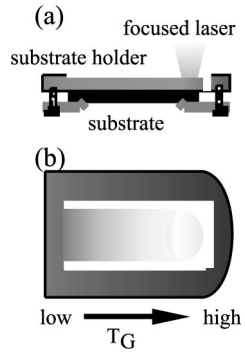

FIG. 8. Schematics of the temperature gradient method: (a) side view and (b) bottom view of the substrate holder. The laser used for heating is focused on one side of the substrate holder. Asymmetric thermal isolation gives a continuous gradient of the temperature.

presence of Ga at the surface facilitates the incorporation of N. This is consistent with the codoping theory.[6]

As shown in Fig. 7, it is difficult to control C_N accurately in the film, because C_N decreases exponentially by orders of magnitude with an increase in substrate temperature. However, it is possible to change C_N systematically for a film on a substrate by creating a controlled temperature gradient[13] on the substrate. A continuous wave semiconductor laser beam was used to irradiate the backside of a substrate holder with an asymmetric thermal isolation profile, as illustrated in Fig. 8. The substrate holder was subjected to a linear temperature gradient within each of the ranges given in Table II, and monitored by a fine focus pyrometer. Simultaneous doping of N and Ga in a ZnO film on a $ScAlMgO_4$ substrate occurred under conditions A–C described in Table II using the alternative pulsed laser ablation technique with two targets under a constant N radical supply. The temperature at the edge of the holder was varied from 410 to 750 °C. Oxygen partial pressures (P_{O_2}) of 1×10^{-5} and 1×10^{-6} Torr were used.

Figures 9(a)–9(c) summarize, respectively, the spread in growth temperature of C_{Ga}, and C_N for about 20 runs of experiments, for which detailed SIMS analyses were carried out. The SIMS measurements were carried out at three to five positions on each sample along the temperature gradient. C_{Ga} can be regulated by the appropriate choice of C_{Ga}^{target} for the target and ablation ratio. However, C_N has a considerable spread depending on the growth temperature, as already indicated in Fig. 7. The resulting C_{Ga} [Fig. 9(b)] is higher by a factor of approximately 2 than C_{Ga}^{calc} (horizontal broken lines). This is partly due to the difference in ablation rate between Ga-doped ceramic ZnO and highly pure EP targets, and partly due to the rather higher vapor pressure of Zn-related species.[14] Although a slight variation of C_{Ga} was observed over the temperature gradient, its range is much narrower than that of the C_N in the films, as shown in Fig. 9(c).

The temperature dependences of C_{Ga} and C_N for the ZnO:(Ga,N) films grown using the temperature gradient method at P_{O_2} 1×10^{-6} and 1×10^{-5} Torr, are shown in Figs. 10(a) and 10(b), respectively. C_{Ga} was not influenced by P_{O_2} and it was constantly regulated at around 10^{18}, 10^{19}, and 10^{20} cm^{-3}. Although nitrogen is more likely to be incorporated into a ZnO film at lower temperatures with a lower P_{O_2} due to the larger amount of nitrogen radical at the growing surface, C_N is predominantly governed by thermally activated desorption of N-related species, regardless of P_{O_2}. C_N for the three kinds of samples grown for each P_{O_2} regime varies over three orders of magnitude from 10^{18} to 10^{21} cm^{-3}, covering the range of control of C_{Ga}. It should be noted that the variation of C_N in each sample crosses the regulated Ga concentration. Figure 10(c) shows the C_N/C_{Ga} ratio for these samples. In practical terms a ZnO:(Ga,N) film grown by pulsed laser deposition can cover a wide range of

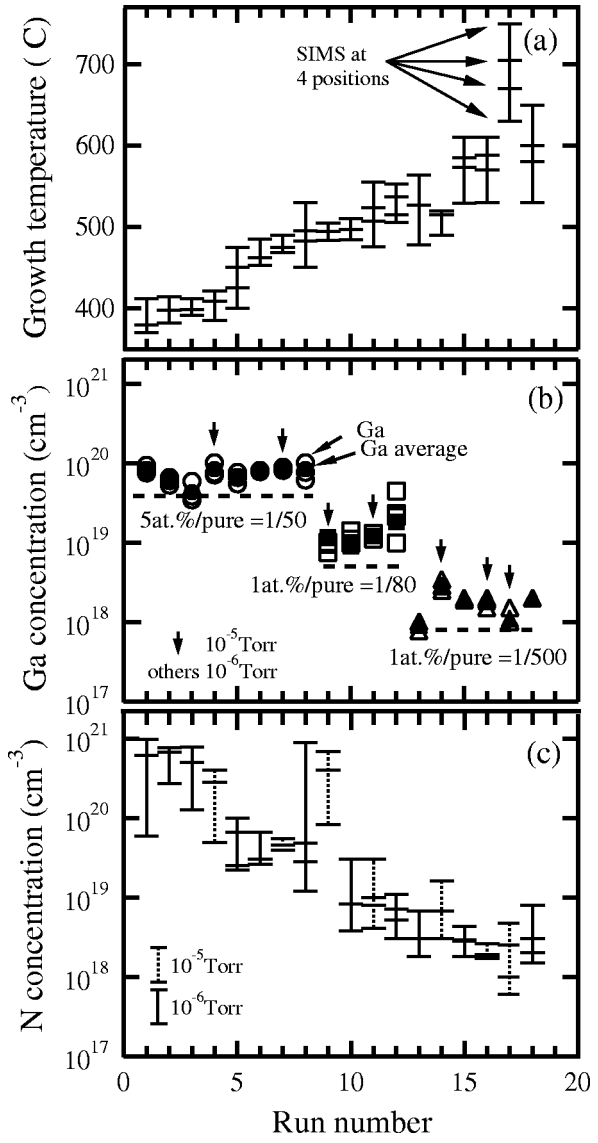

FIG. 9. Summary of SIMS experimental runs for spreads in (a) growth temperature, (b) C_{Ga}, and (c) C_N. In each run, SIMS analysis was made at three or four positions along the temperature gradient, indicated by the ticks on the bars given in (a) and (c). The horizontal dotted lines in (b) indicate the calculated Ga concentration. The nitrogen concentration is given as a continuous spread in the vertical bars in (c) for each run. The circle, square, and triangle in (b) correspond to ablating schemes A, B, and C described in Table II, respectively. The open and closed symbols in (b) are the measured values of C_{Ga} and the average value along the temperature gradient in each of the samples, respectively. The symbols indicated by arrows in (b) and the dotted lines in (c) are for the films grown with P_{O_2}:1×10^{-5} Torr. The other markers in (b) and (c) are for the films grown with P_{O_2}:1×10^{-6} Torr.

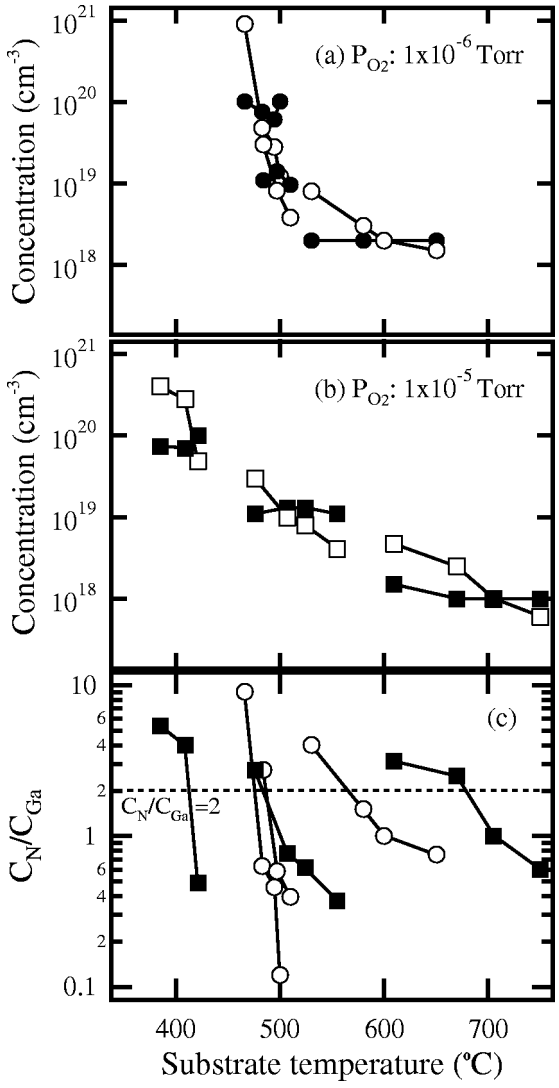

FIG. 10. Temperature dependence of C_N and C_{Ga} in ZnO:(Ga,N) films deposited with (a) P_{O_2}:1×10^{-6} and (b) 1×10^{-5} Torr, using the temperature gradient method. The closed and open symbols represent C_{Ga} and C_N, respectively. (c) C_N/C_{Ga} ratio for the samples deposited with P_{O_2}:1×10^{-6} and 1×10^{-5} Torr represented by open circle and closed square symbols, respectively. All specimens have a position where $C_N/C_{Ga}=2$.

C_N/C_{Ga} ratios, from $C_N/C_{Ga}\gg1$ for lower substrate temperature to $C_N/C_{Ga}\ll1$ for higher substrate temperature, as shown in Fig. 7. In Fig. 10(c), the variation in the ratio occurs in the range of 0.1–10. Since the samples were prepared by the temperature gradient method, continuous variation of C_N/C_{Ga} was achieved in the substrate. Consequently, the samples include a region with the correct concentration ratio of $C_N/C_{Ga}=2$ where *p*-type conduction has been theoretically predicted in ZnO at various C_{Ga} levels from 10^{18} to 10^{20} cm^{-3}. The absence of *p*-type conduction in these samples has already been reported in Ref. 5.

IV. CONCLUSION

We have investigated a technique for analyzing quantitatively heterovalent impurities in ZnO materials by SIMS measurements and have systematically controlled C_N and C_{Ga} in ZnO films grown by pulsed laser deposition. The signal of the negatively charged secondary ion $^{70}Zn^{16}O^-$ ($m/e=86$) should be used as the matrix. When the signals relating to the Ga and N concentrations in the ZnO are to be detected by the SIMS measurement, the use of $^{71}Ga^{16}O^-$ ($m/e=87$) and $^{14}N^{16}O^-$ ($m/e=30$), respectively, are the most reliable secondary ions. The ratios of $^{71}Ga^{16}O^-$ and $^{14}N^{16}O^-$ to $^{70}Zn^{16}O^-$ correspond to the absolute concentration of Ga and N in the ZnO films. Alternating ablation of a single crystal and a ceramic target containing a concentrated Ga dopant allow systematic control of the Ga concentration while at the same time maintaining minimal contamination from undesired impurities. Since C_N and C_{Ga} in a ZnO:(Ga,N) film grown by pulsed laser deposition can be controlled by altering the substrate temperature and the alternative ablation ratio, respectively, high-quality ZnO:(Ga,N) films on $ScAlMgO_4$ substrates with a wide spread in composition for the C_N/C_{Ga} ratio were achieved at various C_{Ga} levels by using the temperature gradient method. The composition-spread sample contained a region with the right ratio ($C_N/C_{Ga}=2$) to satisfy theoretical prediction of *p*-type conduction in ZnO.

ACKNOWLEDGMENT

This work was supported in part by the Collaboration Program of the Institute for Materials Research, Tohoku University.

[1] Z. K. Tang, G. K. L. Wong, P. Yu, M. Kawasaki, A. Ohtomo, H. Koinuma, and Y. Segawa, Appl. Phys. Lett. **72**, 3279 (1998).
[2] A. Ohtomo, K. Tamura, T. Makino, Y. Segawa, Z. K. Tang, K. L. Wong, Y. Matsumoto, H. Koinuma, and M. Kawasaki, Appl. Phys. Lett. **77**, 2204 (2000).
[3] H. D. Sun *et al.*, Appl. Phys. Lett. **77**, 4250 (2000).
[4] K. Ohkawa, T. Karasawa, and T. Mitsuyu, J. Cryst. Growth **117**, 375 (1991).
[5] A. Tsukazaki, H. Saito, K. Tamura, M. Ohtani, H. Koinuma, M. Sumiya, S. Fuke, T. Fukumura, and M. Kawasaki, Appl. Phys. Lett. **81**, 235 (2002).
[6] T. Yamamoto and H. Katayama-Yoshida, Jpn. J. Appl. Phys., Part 2 **38**, L166 (1999).
[7] H. A. Stroms, K. F. Brown, and J. D. Stein, Anal. Chem. **49**, 2023 (1977).
[8] M. Sumiya, K. Yoshimura, K. Ohtsuka, and S. Fuke, Appl. Phys. Lett. **76**, 2098 (2000).
[9] A. Ohtomo, K. Tamura, K. Saikusa, K. Takahashi, T. Makino, Y. Segawa, H. Koinuma, and M. Kawasaki, Appl. Phys. Lett. **75**, 2635 (1999).
[10] S. Ohashi, M. Lippmaa, N. Nakagawa, H. Nagasawa, H. Koinuma, and M. Kawasaki, Rev. Sci. Instrum. **70**, 178 (1999).
[11] J. Lindhard, M. Scharff, and H. E. Schiott, Mat. Fys. Medd. K. Dan. Vidensk. Selsk. **33**, 14 (1963).
[12] K. Tamura *et al.*, J. Cryst. Growth **214/215**, 59 (2000).
[13] A. Tsukazaki, H. Saito, M. Sumiya, K. Tamura, S. Fuke, H. Koinuma, and M. Kawasaki, Proceedings of the 2001 Materials Research Society Fall meeting, 2001.
[14] A. Ohtomo, M. Kawasaki, T. Koida, K. Masubuchi, H. Koinuma, Y. Sakurai, Y. Yoshida, T. Yasuda, and Y. Segawa, Appl. Phys. Lett. **72**, 2466 (1998).